

A New Mechanism for the α to ω Martensitic Transformation in Pure Titanium

D. R. Trinkle,¹ R. G. Hennig,¹ S. G. Srinivasan,² D. M. Hatch,³
M. D. Jones,⁴ H. T. Stokes,³ R. C. Albers,² and J. W. Wilkins¹

¹Ohio State University, Columbus, OH 43210

²Los Alamos National Laboratory, Los Alamos, NM 87545

³Brigham Young University, Provo, UT 84602

⁴State University of New York, Buffalo, NY 14260

(Dated: October 19, 2018)

We propose a new direct mechanism for the pressure driven $\alpha \rightarrow \omega$ martensitic transformation in pure titanium. A systematic algorithm enumerates all possible mechanisms whose energy barriers are evaluated. A new, homogeneous mechanism emerges with a barrier at least four times lower than other mechanisms. This mechanism remains favorable in a simple nucleation model.

PACS numbers: 81.30.Kf, 64.70.Kb, 5.70.Fh

Martensitic transformations are abundant in nature and are commonly used in engineering technologies [1]. Materials from steel to shape-memory alloys are governed by their underlying martensitic transformations [2]. The pressure driven α (hcp) \rightarrow ω (hexagonal) transformation in pure titanium, discussed here and reviewed extensively by Sikka *et al.* [3], has significant technological implications in the aerospace industry because the ω phase formation lowers toughness and ductility. This transformation was first observed by Jamieson [4], and has since been extensively studied using static high-pressure [5] and shockwave methods [6]. Because of experimental difficulties in directly observing martensitic transformation mechanisms, they are usually inferred from the orientation relationships between the initial and final phases. Such an approach may result in multiple transformation mechanisms for any given set of orientation relations, and requires one to guess the appropriate transformation mechanism. Thus, despite several attempts, the mechanism for this transformation is still unclear.

We calculate the energy barrier for homogeneous transformation for different titanium $\alpha \rightarrow \omega$ transformation mechanisms and compare the values using a simplified nucleation model. We systematically generate and sort possible $\alpha \rightarrow \omega$ mechanisms by their energy barriers. A new direct mechanism emerges whose barrier is lowest both homogeneously and when considered in a simple nucleation model.

Figure 1 shows our new low energy barrier mechanism for the $\alpha \rightarrow \omega$ transformation in Ti, called TAO-1, for “Titanium Alpha to Omega.” This direct 6-atom transformation requires no intermediary phase, and has small shuffles and strains. The 6 atoms divide into a group of 4 atoms that shuffle by 0.63 Å and 2 atoms that shuffle by 0.42 Å. Combining these shuffles with strains of $\varepsilon_x = 0.91$, $\varepsilon_y = 1.12$, and $\varepsilon_z = 0.98$ produces a final ω cell from our α cell. The original α matrix is then oriented relative to the ω matrix such that $(0001)_\alpha \parallel (0\bar{1}11)_\omega$ and $[11\bar{2}0]_\alpha \parallel [01\bar{1}1]_\omega$. These orientation relations are seen in

some experiments, but not others [5, 6, 7].

Our mechanism identification method matches possible supercells of α and ω to determine the lattice strain, and atom positions to determine the necessary internal relaxations; similar to [8]. While there are infinitely many possible supercells, we consider only 6 and 12 atom supercells with principal strains less than 1.333 and greater than $0.75 = 1.333^{-1}$. For each supercell, there are multiple ways to shuffle the atom positions from α to ω ; we consider mechanisms where, relative to the center of mass, no atom moves more than 2.0 Å. We also limit the closest distance of approach between any two atoms during the transformation. Each supercell has one mechanism with the largest closest approach distance; we consider all mechanisms for that supercell within 0.1 Å of that value.

To efficiently compare the enthalpy barriers of the possible mechanisms, we use three methods of increasing computational sophistication and accuracy. **1.** For each mechanism, we calculate an approximate barrier based only on the strain, using the elastic approximation. Such a calculation of the “elastic barrier” relies only on the elastic constants for each phase, and the supercell geometry [20]. **2.** For mechanisms with a low elastic barrier, we calculate an energy landscape using a strain variable (ε) and a single concerted shuffle variable (δ). The energies $E(\varepsilon, \delta)$ are calculated using a tight-binding (TB) model [10] on a grid between α at $E(0,0)$ and ω at $E(1,1)$. The energy at the transition state in this reduced space gives a “landscape barrier.” **3.** For mechanisms with the lowest landscape barriers, we calculate the exact barrier using the nudged elastic band (NEB) method [11] together with our TB model [10] or *ab initio* VASP simulations [12], or both. During the NEB calculation, the cell shape and size are allowed to change in response to the applied pressure. In general, we expect the elastic barrier to underestimate the TB landscape barrier, and the TB landscape barrier to overestimate the TB-NEB barrier. The most probable mechanism should have the smallest *ab initio* NEB enthalpy barrier.

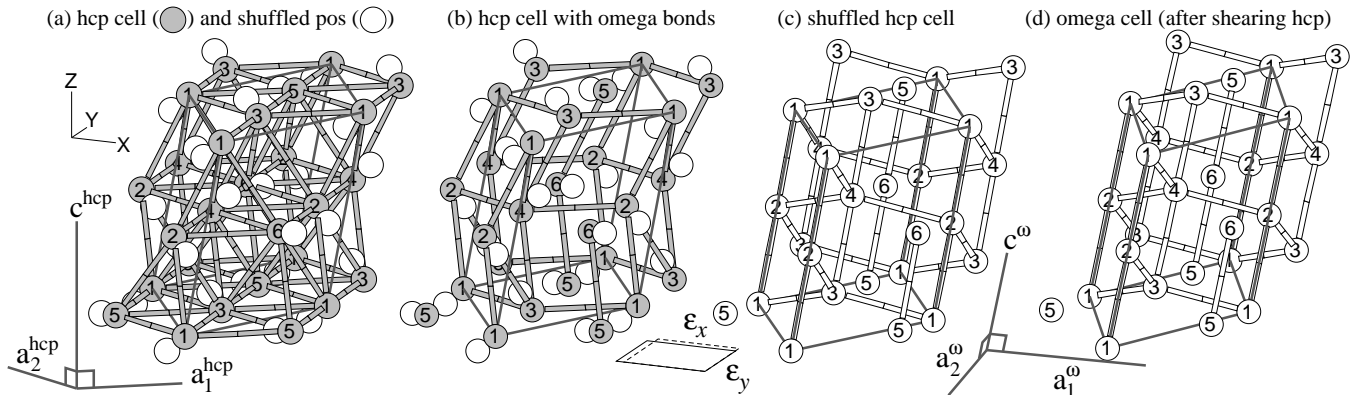


FIG. 1: Our proposed $\alpha \rightarrow \omega$ transformation mechanism (TAO-1). The direct 6-atom transformation is visualized (i) as a two-step process, (ii) with 21 additional atoms outside the heavy gray parallelepiped supercell. In α , atoms 1,3,5 and 2,4,6 are in the A and B stacking planes, respectively; whereas in ω , atoms 1–4 are in the Wyckoff d position of space group $P6/mmm$, and atoms 5–6 are in the Wyckoff a position [9]. (a) The grey atoms in the α cell shuffle to new positions (white atoms), with atoms 1–4 shuffling 0.63 Å, and atoms 5–6 shuffling 0.42 Å. (b) The α cell is redrawn with the “bonds” of the ω structure. **Step 1:** Shuffling the grey atoms to the white positions, the α cell (b) produces a strained ω cell (c), contained in the same supercell. **Step 2:** Straining the supercell (c) $\epsilon_x = 0.91$, $\epsilon_y = 1.12$, and $\epsilon_z = 0.98$ produces the final ω supercell (d). The orientation relations connecting the α and ω supercells are: $(0001)_\alpha \parallel (0\bar{1}11)_\omega$ and $[11\bar{2}0]_\alpha \parallel [01\bar{1}1]_\omega$.

We calculate total energies using a TB model and carefully converged *ab initio* calculations. The TB calculations are performed with OHMMS [13] and use Mehl and Papaconstantopoulos’s functional form [10] with parameters that are refit to reproduce LAPW total energies for hcp, bcc, fcc, omega, and sc to within 0.5 meV/atom. For each mechanism, we use a k-point mesh equivalent to $12 \times 12 \times 8$ in hcp with a 63 meV thermal smearing to give an energy convergence of 1 meV/atom. For our *ab initio* calculations [21] we include $3p$ electrons in the valence band, and use a plane-wave kinetic-energy cutoff of 400 eV and a $7 \times 7 \times 7$ k-point mesh to ensure energy convergence to within 1 meV/atom. We relax the atomic positions and the unit cell shape and volume until the total electronic energy changes by less than 1 meV.

The elastic and landscape energy barrier calculations reduce our initial set of 977 candidate mechanisms to the 3 lowest barrier mechanisms. From the initial list of 134 supercells, we reject all but 57 because their elastic barriers are large (greater than 100 meV/atom). For the remaining 57 supercells, we generate 977 mechanisms (6 6-atom mechanisms and 971 12-atom mechanisms), and compute TB landscape barriers. Figure 2 shows that the elastic barrier underestimates the landscape barrier. We select the three mechanisms with the smallest landscape barriers—TAO-1, TAO-2, and Silcock—for careful study.

Figure 3 illustrates the Silcock mechanism [14]. Her mechanism, determined from observed orientation relations, involves significant atomic shuffle, relatively small strains, and is a direct transformation mechanism with no intermediate state. In each α stacking plane, 3 out of every 6 atoms shuffle by 0.74 Å along $[11\bar{2}0]_\alpha$, while the other 3 shuffle in the opposite direction $[\bar{1}120]_\alpha$. This shuffle is accompanied by a strain $\epsilon_x = 1.05$ along $[1\bar{1}00]_\alpha$

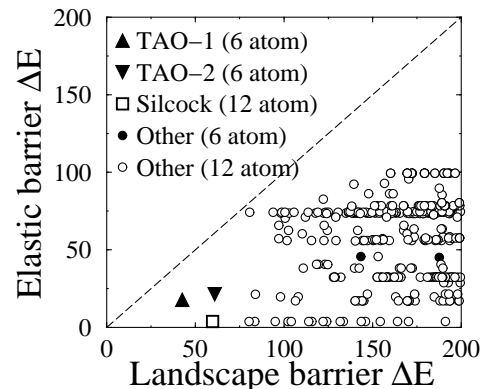


FIG. 2: Approximate elastic energy barrier (meV/atom) versus landscape energy barrier (meV/atom) for 359 mechanisms whose landscape barrier is below 200 meV/atom. Of the 134 supercells generated, 57 had low (less than 100 meV/atom) elastic barriers. From those 57 supercells, 977 mechanisms were generated; for those 977 mechanisms, we calculate a shear/shuffle energy landscape using our tight-binding parameters. Of those 977, 359 mechanisms had an elastic barrier below 200 meV/atom. We select the three mechanisms in the bottom left corner—TAO-1, TAO-2, and Silcock—and calculate their true barrier using the *ab initio* NEB method.

and $\epsilon_y = 0.95$ along $[11\bar{2}0]_\alpha$ to produce a hexagonal ω cell with the correct c/a ratio. Despite the lack of direct conclusive evidence to support the Silcock mechanism, it is still widely invoked to describe the $\alpha \rightarrow \omega$ transformation because it is a direct mechanism [15].

The remaining two mechanisms, TAO-1 and TAO-2, are related to Usikov and Zilbershtein’s [7] proposed composite mechanism involving the thermodynamically unstable β (bcc) intermediary phase, and proceeding as

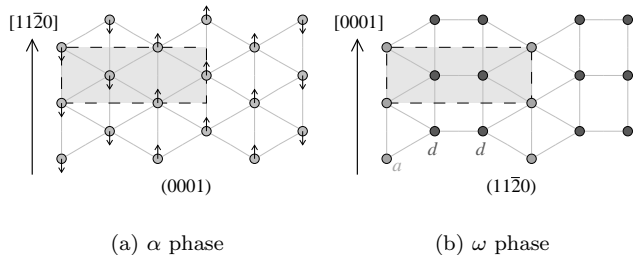


FIG. 3: Silcock mechanism for α to ω transformation (single α stacking plane shown). (a) In each stacking plane, 3 out of every 6 atoms shuffle by 0.74 \AA along $[11\bar{2}0]_{\alpha}$, while the other 3 shuffle in the opposite direction $[\bar{1}\bar{1}20]_{\alpha}$. (b) This creates the $(11\bar{2}0)_{\omega}$ plane from $(0001)_{\alpha}$. The a and d Wyckoff positions of $P6/mmm$ are also shown. This shuffle is accompanied by a strain $\varepsilon_x = 1.05$ along $[1\bar{1}00]_{\alpha}$ and $\varepsilon_y = 0.95$ along $[11\bar{2}0]_{\alpha}$ to produce a hexagonal ω cell with the correct c/a ratio. The orientation relations connecting the α and ω supercells are: $(0001)_{\alpha} \parallel (11\bar{2}0)_{\omega}$ and $[11\bar{2}0]_{\alpha} \parallel [0001]_{\omega}$.

$\alpha \rightarrow \beta \rightarrow \omega$. Using the α - ω orientation relations, they proposed an $\alpha \rightarrow \beta$ transformation via an inverse Burgers mechanism [16] followed by a $\beta \rightarrow \omega$ transformation via the collapse of 2 out of 3 $(111)_{\beta}$ planes. This produced two unique mechanisms, called Variant I and Variant II, depending on the direction of $\{111\}_{\beta}$ planes to collapse. The TAO-1 and TAO-2 mechanisms could have been constructed from Variant I and II, respectively, by using the β intermediate system to construct a 6 atom supercell. Allowing Variant I and II to relax away from the β phase would have resulted in direct transformation mechanisms.

Table I summarizes the energy barriers for the three mechanisms of interest and identifies TAO-1 as having the lowest energy barrier. The TAO-1 mechanism provides the best trade off between shuffle and strain; during the transformation, the closest nearest neighbor distance is 2.63 \AA , which is larger than the 2.55 \AA value for TAO-2 and 2.57 \AA for Silcock. Because the nearest-neighbor distances in α and ω are 2.95 \AA and 2.65 \AA , respectively, it is not surprising that TAO-1 has the lowest barrier. The barrier to pass through the intermediate β phase, as suggested by Usikov and Zilbershtein [7], is 108 meV/atom —drastically larger than TAO-1’s barrier of 9 meV/atom .

Figure 4 shows the enthalpy along the $\alpha \rightarrow \omega$ transformation path for the three mechanisms as a function of pressure. Our calculation shows ω slightly lower in energy than α at 0 GPa. The crystal structure at 0 K has not been determined experimentally; however, extrapolation of the α - ω phase boundary indicates ω as the ground state [3]. As pressure increases, the enthalpy of ω relative to α drops, and all three mechanisms decrease their enthalpy barrier. For the next four lowest landscape barrier mechanisms in Figure 2, we find 0 GPa *ab initio* NEB

TABLE I: Comparison of TAO-1, TAO-2, and Silcock mechanisms. Energy barriers: Four different methods for calculating the energy barrier for the three mechanisms are shown, from least accurate to most accurate. The elastic barrier only accounts for the strain in each mechanism. The landscape barrier uses a simple combined shuffle for each, and a tight-binding total energy. Finally, the NEB calculation is done with the tight-binding method and *ab initio* to accurately determine the barrier. Orientation Relations: The relative orientation of α to ω is shown for each mechanism. N.B.: Silcock and TAO-2 mechanisms have the same orientation relations.

	TAO-1	TAO-2	Silcock
Homogeneous barriers (in meV/atom)			
Elastic barrier:	18	21	3.7
Landscape barrier:	41	59	59
TB-NEB barrier:	24	52	54
<i>ab initio</i> NEB barrier:	9	58	31
Transformation information			
Orientation	$(0001)_{\alpha} \parallel (0\bar{1}11)_{\omega}$	$(0001)_{\alpha} \parallel (11\bar{2}0)_{\omega}$	
Relations:	$[11\bar{2}0]_{\alpha} \parallel [01\bar{1}1]_{\omega}$	$[11\bar{2}0]_{\alpha} \parallel [0001]_{\omega}$	

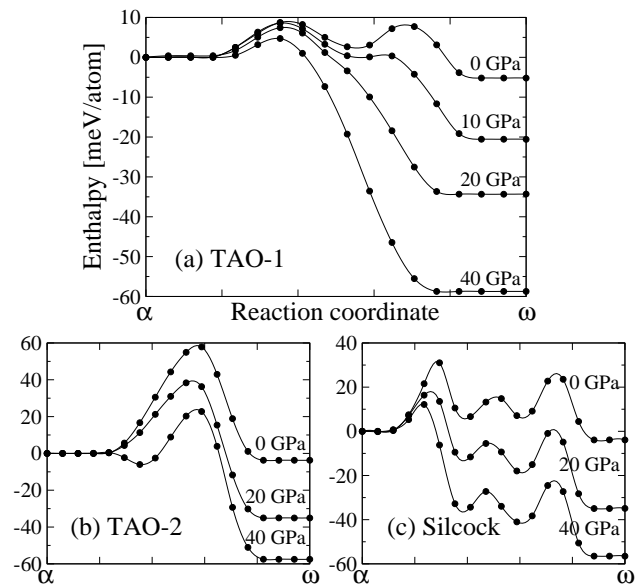


FIG. 4: Enthalpy barrier vs. pressure for the three lowest energy mechanisms, using *ab initio* NEB at 16 intermediate states. The *ab initio* NEB gives the $T = 0$ energy along the homogeneous $\alpha \rightarrow \omega$ pathway for each mechanism. The enthalpy barriers decrease with increasing pressure. (a) The TAO-1 mechanism gives the smallest barrier by a factor of 4 at 0 GPa. The TAO-2 mechanism (b) and Silcock mechanism (c) have larger barriers at 0 GPa; an ordering which continues even at 40 GPa.

barriers of 32, 37, 68, and 69 meV/atom. The barrier of the TAO-1 mechanism is lowest, even up to 40 GPa.

We use classical nucleation theory to relate the homogeneous barriers to the energy scales relevant for microscopic transformation mechanics, given by the formation energy of a critical nucleus. If the formation energy of the critical nuclei is of the same order as the barrier, our

mechanism prediction is not expected to change. In classical nucleation theory, nuclei of new material grow only if they are larger than a critical size where the nucleation energy is an extrema. The nucleation energy consists of three terms: the interfacial energy, the enthalpy difference, and the stress from the volume difference.

In estimating the energy to create the critical nucleus, we use the α -Ti surface energy of 125 meV/Å² as an upper bound for the α - ω interfacial energy. The enthalpy difference at the experimental shock transition pressure of 10 GPa is -20 meV/atom, and the stress from the volume difference is 3.5 meV/atom. We use the same critical nucleus size for each mechanism in Table I because they each have a plane with no strain after the transformation, so the nuclei likely grow as oblate spheroids to minimize stress. Classical nucleation theory estimates a critical nucleus radius of 240 Å, (3.5 million atoms) with a formation energy of 30 keV. For that sized nucleus the 9 meV/atom barrier of TAO-1 becomes a homogeneous barrier of 28 keV. In contrast, the competing TAO-2 and Silcock mechanisms have barriers of 200 and 120 keV respectively; far above the formation energy and the TAO-1 barrier.

Our systematic search, involving both tight-binding and *ab initio* calculations, combined with a nucleation analysis leads to the direct TAO-1 mechanism as the preferred $\alpha \rightarrow \omega$ mechanism in pure titanium. Our approach allows us to find the lowest barrier mechanism for any martensitic phase transformation by generating and comparing all relevant possible mechanisms. Indeed this method provides an invaluable starting point for investigating any martensitic transformation.

Acknowledgments. We thank G. T. Gray III and C. W. Greeff for helpful discussions, and M. I. Baskes and R. B. Schwarz for reviewing the manuscript. DRT thanks Los Alamos National Laboratory for its hospitality and was supported by a Fowler Fellowship at Ohio State University. This research is supported by DOE grants DE-FG02-99ER45795 (OSU) and W-7405-ENG-36 (LANL). Computational resources were provided by the Ohio Supercomputing Center and NERSC.

[1] *Martensite*, eds. G. B. Olson and W. S. Owen (ASM, 1992), 1.
 [2] *Shape Memory Materials*, eds. K. Otsuka and C. M. Wayman (Cambridge University Press, 1998), 1.
 [3] S. K. Sikka, Y. K. Vohra, and R. Chidambaram, *Prog. Mater. Sci.* **27**, 245 (1982).
 [4] J. C. Jamieson, *Science* **140**, 72 (1963).
 [5] A. Jayaraman, W. Klement Jr., and G. C. Kennedy, *Phys. Rev.* **131**, 644 (1963); V. A. Zilbershtein, G. I. Nosova, E. I. Estrin, *Fiz. Metal. Metalloved* **35**, 584 (1973); Y. K. Vohra, S. K. Sikka, S. N. Vaidya, and

R. Chidambaram, *J. Phys. Chem. Solids* **38**, 1293 (1977); H. Xia, G. Parthasarathy, H. Luo, Y. K. Vohra, and A. L. Ruoff, *Phys. Rev. B* **42**, 6736 (1990); Y. K. Vohra and P. T. Spencer, *Phys. Rev. Lett.* **86**, 3068 (2001).
 [6] R. G. McQueen, S. P. Marsh, J. W. Taylor, J. N. Fritz, and W. J. Carter in *High-velocity Impact Phenomenon*, ed. R. Kinslow (Academic Press, New York and London, 1970), 293; A. R. Kutsar, V. N. German, and G. I. Nasova, *Dokl. Akad. Nauk, SSSR* **213**, 81 (1973); G. T. Gray III, C. E. Morris, and A. C. Lawson in *Titanium 1992—Science and Technology*, eds. F. H. Froes and I. L. Caplan (Warrendale, PA: TMS, 1993), 225; S. V. Razorenov, A. V. Utkin, G. I. Kanel, V. E. Fortov, and A. S. Yarunichev, *High Pressure Research* **13**, 367 (1995); R. F. Trunin, G. V. Simakov, and A. B. Medvedev, *High Temperature* **37**, 851 (1999); C. W. Greeff, D. R. Trinkle, and R. C. Albers, *J. Appl. Phys.* **90**, 2221 (2001).
 [7] M. P. Usikov and V. A. Zilbershtein, *Phys. Stat. Sol. (a)* **19**, 53 (1973).
 [8] H. T. Stokes and D. M. Hatch, *Phys. Rev. B* **65**, 144114 (2002); S. G. Srinivasan, D. M. Hatch, H. T. Stokes, A. Saxena, R. C. Albers, and T. Lookman, *cond-mat/0209530*.
 [9] *International Tables for Crystallography, Vol. A*, ed. T. Hahn (Kluwer Academic, London, 2002).
 [10] M. J. Mehl and D. A. Papaconstantopoulos, *Phys. Rev. B* **54**, 4519 (1996); M. J. Mehl and D. A. Papaconstantopoulos, *cond-mat/0111180* (2002); D. R. Trinkle, R. G. Hennig, M. D. Jones, D. M. Hatch, S. G. Srinivasan, H. T. Stokes, R. C. Albers, and J. W. Wilkins, (unpublished).
 [11] H. Jónsson, G. Mills, and K. W. Jacobsen, in *Classical and Quantum Dynamics in Condensed Phase Simulations*, eds. B. J. Berne, G. Cicciotti, and D. F. Coker (Singapore: World Scientific, 1998), 385.
 [12] G. Kresse and J. Hafner, *Phys. Rev. B* **47**, RC558 (1993); G. Kresse and J. Furthmüller, *Phys. Rev. B* **54**, 11169 (1996).
 [13] J. N. Kim (private communication).
 [14] J. M. Silcock, *Acta Metall.* **6**, 481 (1958); sometimes attributed to A. Rabinkin, M. Talianker, and O. Botstein, *Acta Metall.* **29**, 691 (1981).
 [15] A. V. Dobromyslov and N. I. Taluts, *Phys. Met. Metall.* **69**, 98 (1990); H. Dannak, A. Dunlop, and D. Lesueur, *Phil. Mag. A* **79**, 147 (1999).
 [16] W. G. Burgers, *Physica* **1**, 561 (1934).
 [17] D. Vanderbilt, *Phys. Rev. B* **41**, 7892 (1990).
 [18] G. Kresse and J. Hafner, *J. Phys.: Cond. Mat.* **6**, 8245 (1994).
 [19] J. P. Perdew and Y. Wang, *Phys. Rev. B* **45**, 13244 (1992).
 [20] If $E_{s-\alpha}$ and $E_{s-\omega}$ are the energies of the fully strained α and ω within the elastic approximation, the elastic barrier is $E_{s-\alpha}E_{s-\omega}/(E_{s-\alpha}^{1/3} + E_{s-\omega}^{1/3})^3$.
 [21] VASP [12] is a plane-wave based code using ultra-soft Vanderbilt type pseudopotentials [17] as supplied by G. Kresse and J. Hafner [18]. The calculations were performed using the generalized gradient approximation of Perdew and Wang [19].